

## Stacking-fault energy effect on zero-strain deformation twinning in nanocrystalline Cu–Zn alloys



X.L. Ma<sup>a</sup>, H. Zhou<sup>a,b</sup>, J. Narayan<sup>a</sup>, Y.T. Zhu<sup>a,c,\*</sup>

<sup>a</sup> Department of Materials Science and Engineering, North Carolina State University, Raleigh, NC 27695, USA

<sup>b</sup> National Engineering Research Center of Light Alloy Net Forming, Shanghai Jiao Tong University, Shanghai 200240, China

<sup>c</sup> School of Materials Science and Engineering, Nanjing University of Science and Technology, Nanjing 210094, China

### ARTICLE INFO

#### Article history:

Received 11 May 2015

Revised 15 July 2015

Accepted 21 July 2015

Available online 29 July 2015

#### Keywords:

Deformation twin

Zero-strain twinning

Nanocrystalline alloy

Stacking-fault energy

### ABSTRACT

It has been reported that most deformation twins in nanocrystalline face-centered-cubic metals do not produce macroscopic strain. Here we report the decrease of zero-strain deformation twinning with decreasing stacking-fault energy. One of the two major mechanisms that produce zero-strain twinning is cooperative slip of three partials under external applied stress. Lower stacking-fault energy weakens this mechanism and statistically reduces the fraction of twins with zero-strain.

Published by Elsevier Ltd. on behalf of Acta Materialia Inc.

In conventional coarse-grained metals, deformation twinning is usually accompanied by macroscopic strain [1,2]. This was considered a characteristic of twinning for over half century because all of the conventional twinning mechanisms in coarse-grained materials, including pole, prismatic glide, faulted dipole, etc. require the slips of twinning partials with the same Burgers vector on consecutive slip planes [3–5]. As a result, deformation twinning always generates a macroscopic strain. Recently, zero-strain deformation twinning has been widely found in nanocrystalline (NC) face-centered-cubic (FCC) metals and alloys and even in a few coarse-grained materials [6–11]. Zero-strain twins are generated via twinning partials with different Burgers vectors, whose sum is zero [2]. They could affect the mechanical behavior and microstructural evolution of NC metals. For example, instead of locally accumulating macroscopic strain in twinned grains, zero-strain twins participate in plastic deformation by re-orienting the lattice without producing jagged grain boundaries, which makes it easy for grains to rotate and slide during further deformation [6]. Another salient feature of zero-strain twins is the easy migration of incoherent twin boundaries (ITBs) under slight external stress [7,12]. This feature is believed to play a critical role in strain softening [13,14].

Two major mechanisms have been proposed for deformation twinning with zero-strain in NC FCC metals. Wu et al. proposed that random activation of partials (RAP) was the mechanism for their observation of zero-strain twins in severely deformed NC metals such as Ni, Cu and Al [6,15]. It was hypothesized that Shockley partials were individually activated on neighboring slip planes. Due to the random nature of the partials, the sum of their Burgers vectors is close to zero. Experimental observations and molecular dynamics simulations revealed another important mechanism, named as cooperative slip of three partials (CSTP), which generates a twin by cooperative slip of three different partials on three adjacent planes [7,12,16,17], where  $\mathbf{b}_1 + \mathbf{b}_2 + \mathbf{b}_3 = \mathbf{0}$ . The twin propagates through the movement of the  $\Sigma 3\{112\}$  ITBs controlled by the stress balance between each set of three partials, which is simply called the “move-drag” mechanism. Specifically, one or two partials are driven by applied stress while the rest is dragged along due to the stacking-fault energy (SFE) and/or twin fault energy. Both mechanisms were found to play a significant role in zero-strain twinning in NC Cu, which has medium stacking fault energy [10].

In the CSTP mechanism, SFE is assumed to play a critical role while the RAP mechanism is not affected much. However, their comprehensive influence on zero-strain twinning has not been experimentally investigated. The objective of this study is to systematically investigate the SFE effect on zero-strain twinning and the underlying mechanism. Alloying is an effective approach to change SFE [18]. Cu–Zn alloys are selected for this study.

\* Corresponding author at: Department of Materials Science and Engineering, North Carolina State University, Raleigh, NC 27695, USA.

E-mail address: [ytzhu@ncsu.edu](mailto:ytzhu@ncsu.edu) (Y.T. Zhu).

Commercial Cu-10 wt.% Zn, Cu-15 wt.% Zn and Cu-30 wt.% Zn plates were punched into  $\phi$ -10 mm disks, which were subjected to high-pressure torsion (HPT) for 6 revolutions under the same pressure of 1 GPa at 1.5 rpm. Transmission electron microscopy (TEM) foils were made from the very edge of the HPT-processed disks. Each TEM foil was ion milled under the protection of liquid nitrogen. The temperature was set at  $-100$  °C to prevent potential grain growth. Statistical analysis of macroscopic strains and thicknesses of deformation twins was conducted by high-resolution transmission electron microscopy (HRTEM) observation of at least 170 grains in each sample. The average grain size is 40–50 nm for all samples [19]. Vickers micro-hardness tests were performed to estimate the applied stress in each sample.

The morphology of a grain boundary (GB) segment intercepted by a deformation twin is a good indicator on whether a twin produces strain [2]. Smooth GB implies a net zero macroscopic strain and vice versa. A few other factors including GB shuffling and free volume migration may also affect the GB smoothness. However, those factors are assumed to play a minor role in GB-twin interception smoothness and to behave in an unbiased way and therefore do not hinder our statistical study here. Fig. 1 shows typical structures of GBs intercepted by deformation twins. GBs with kinks correspond to twins that produce macroscopic strain, while those without kinks correspond to zero-strain twins. Fig. 1a–c clearly

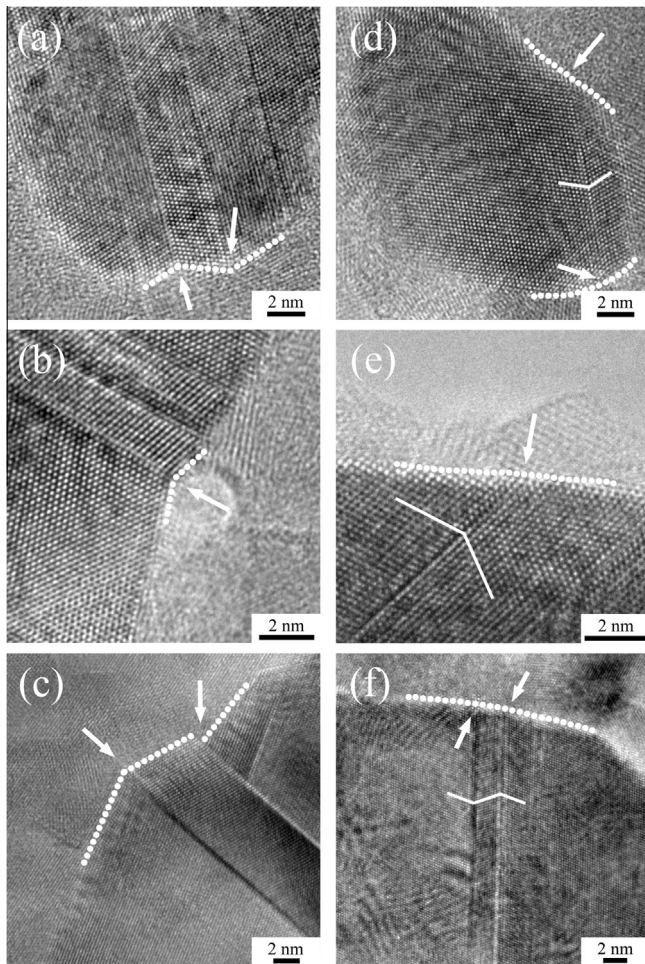
show grain-boundary kinks in three Cu–Zn alloys (marked by dots and arrows). The various kink angles depend on both the view orientations under TEM and the sum of Burgers vectors for the partials that contribute to the twin formation [2]. As seen in Fig. 1d–f, zero-strain twins are also observed in all NC alloys, which are consistent with early reports [8–10].

Statistical analysis shows the fractions of twins with strain and zero-strain twins in Fig. 2a. As shown, zero-strain twins outnumber twins with strain in the Cu–10Zn sample whereas the opposite is true in the Cu–30Zn sample. In other words, the fraction of zero-strain twins is reduced in the low-SFE NC Cu–30Zn alloy (Fig. 2b).

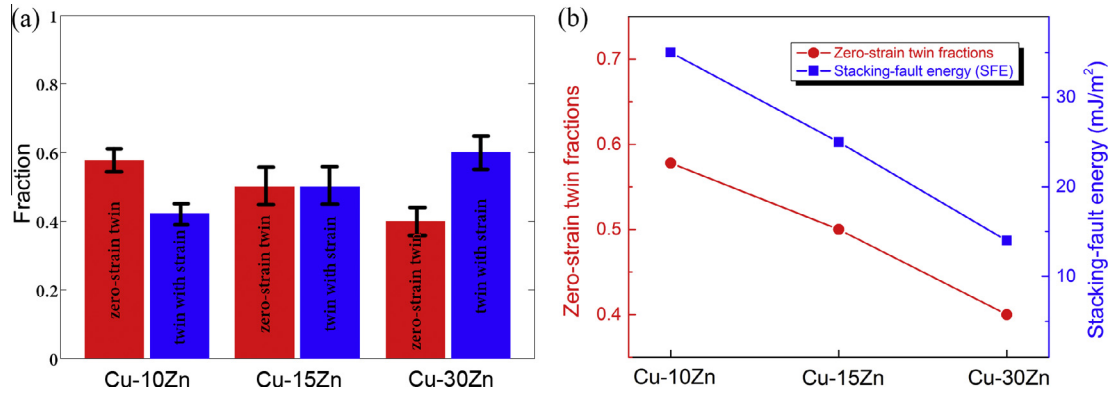
For those zero-strain deformation twins, their ITBs terminated in the grain interior indicate how they were generated [12,17,20]. The CSTP mechanism is operated by cooperative slip of three partials ( $b_1$ ,  $b_2$  and  $b_3$ ) on three slip planes. This feature gives rise to  $\Sigma 3\{112\}$  ITBs with periodic atomic structures, as shown in Fig. 3a. In contrast, another kind of ITB is shown in Fig. 3b. This ITB is not periodic in atomic structure, which is probably generated by the RAP mechanism because RAP randomly generates the partials. Analysis of such ITB structures is helpful to understand the fundamentals of how intrinsic properties and extrinsic conditions affect the formation of zero-strain twins, especially for CSTP twins.

Fig. 3c–e are HRTEM images of ITBs with the CSTP feature in Cu–10Zn. Such features are also present in other two alloys. During the twin propagation,  $\Sigma 3\{112\}$  ITB is split and a periodic atomic sequence is generated due to the local stress balance [16], which is identified by the extra spots in corresponding fast Fourier transforms (FFT) (inset of Fig. 3e) compared to typical FCC  $\langle 110 \rangle$  pattern. By carefully locating the exact ITBs (marked by dotted lines), we measured the split length and found that it varies from twin to twin. When free of local stress, the near-equilibrium length should not be too different from that of pure Cu, which is 0.8 nm [9,12]. This is consistent with what is shown in Fig. 3c with a split length of only 0.88 nm. However, this split length is susceptible to local stress fluctuation. Much longer split lengths such as 3.7 nm and 18.3 nm are shown in Fig. 3d and e. It's noteworthy that 18.3 nm is much longer than previous observations [7,9] in Cu alloys and may represent an extreme case. More importantly, such evidence is a strong clue to even more extreme cases: breakdowns of ITB equilibrium. This is a reasonable hypothesis in our samples during severe plastic deformation, which is also verified by applied stress estimation later.

Fig. 4a–c are schematic illustrations of the breakdown process of  $\Sigma 3\{112\}$  ITB, a possible mechanism to explain the shrinkage of zero-strain twin proportion in low-SFE samples. At stage A, energetic GBs of nano-grains caused by severe plastic deformation nucleate a twin readily and a temporary near-equilibrium ITB is generated at the twin front. The unstable SFE, another critical factor to partial nucleation, doesn't affect this process much because the non-equilibrium GBs contain dissociated dislocations already [21]. Stage B depicts the stable propagation of this twin frontier under appropriate external stress. During this stage, one or two partials (taking  $b_1$  for example and hereafter named as leading partial) moved ahead to propagate the twin. There are two major constraint forces against the separation of this leading partial from the other two: interaction between partials with different Burgers vectors and the SFE. Obviously, the longer the split length of ITB is, the weaker the attraction is from the other two partials. Therefore, stacking fault constraint (blue lines) plays a more important role in balancing ITB as the split length becomes larger. Lower SFE will decrease the mutual constraint within each tri-layer and may destroy the stress quasi-equilibrium. In addition, if the grain size is reduced to nano scale and comparable to the split length, it'll open up more possibilities for the breakdown of ITB equilibrium.



**Fig. 1.** Typical high-resolution TEM images of deformation twins with macroscopic strains in NC (a) Cu–10Zn, (b) Cu–15Zn, (c) Cu–30Zn and zero-strain twins in (d) Cu–10Zn, (e) Cu–15Zn, (f) Cu–30Zn. Solid lines mark the matrix–twin relationships. The twin–GB interceptions are highlighted to indicate the macroscopic strain or the lack of it.



**Fig. 2.** (a) Fraction of zero-strain deformation twins in each Cu–Zn alloy. Red bars stands for fraction of zero-strain twins and blue bars stands for twins with macroscopic strain. (b) Fractions of zero-strain deformation twins and stacking-fault energy (blue) in Cu–Zn alloys. (For interpretation of the references to color in this figure legend, the reader is referred to the web version of this article.)

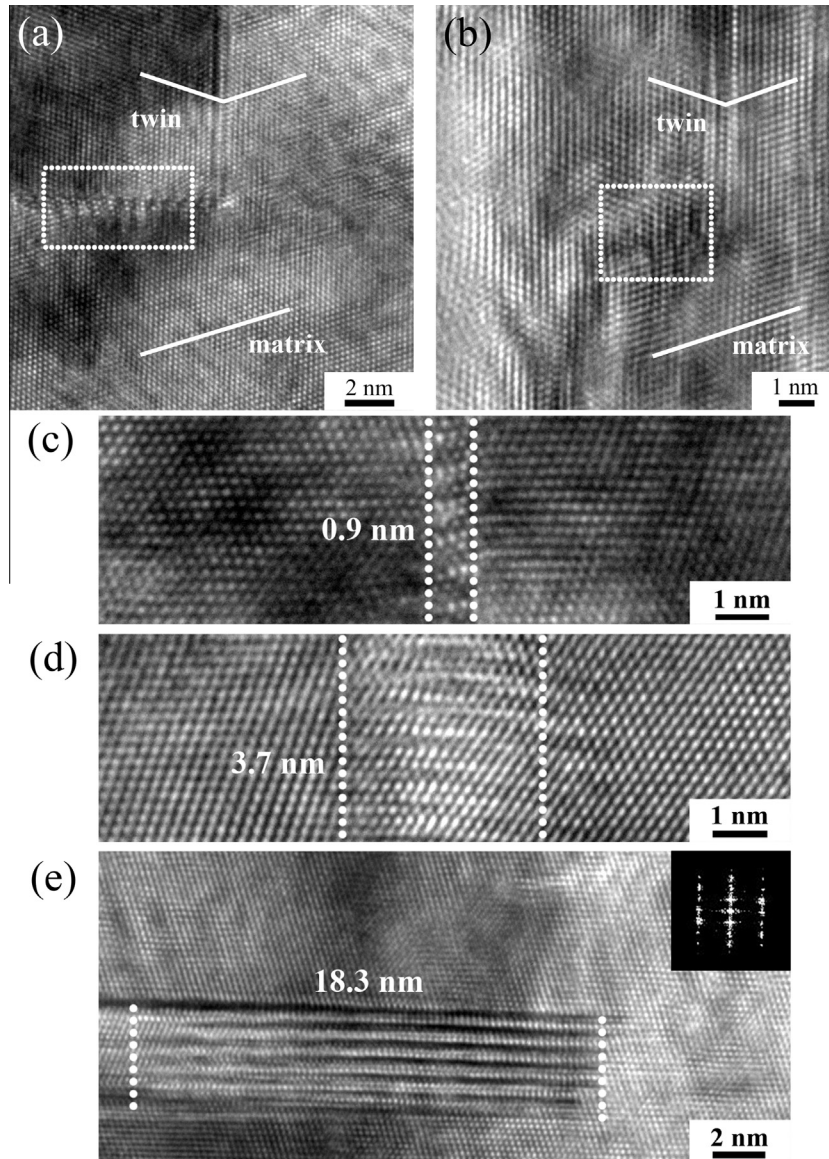


**Fig. 3.** Typical atomic morphology of ITBs of zero-strain twins in the Cu–10Zn alloy: (a) with periodicity:  $\Sigma 3\{112\}$  ITB, (b) without periodicity. Split of  $\Sigma 3\{112\}$  ITBs under (c) near zero stress to (d and e) lower residual stress under equilibrium states in as-deformed nano-grains. Inset in (e) is FFT pattern for the extended ITB, confirming the existence of periodic structure by extra spots.

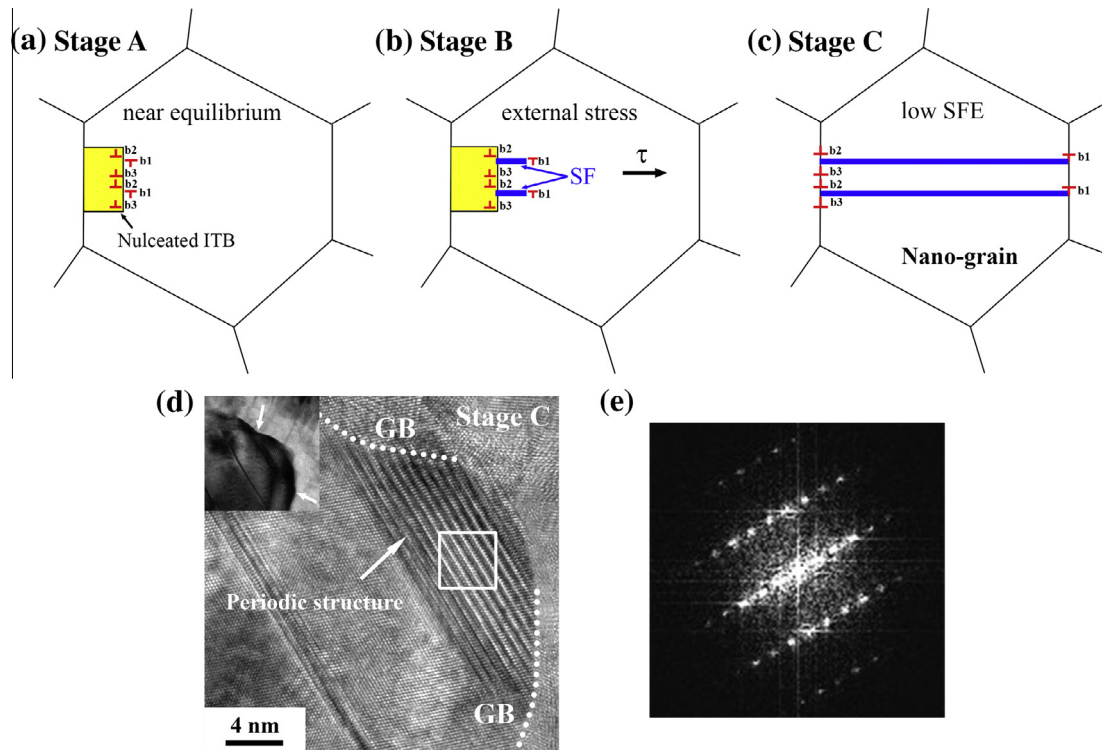


**Fig. 4.** (a–c) Schematic illustration of breakdown process of  $\Sigma 3\{112\}$  ITB in nano-grain FCC materials with low SFE. (d) HRTEM observation of periodic structure at GBs of both ends in the Cu–10Zn alloy. Inset is the low magnified GB image to show the macroscopic strain. (e) FFT result of the selected region in (d), showing the same pattern in Fig. 3e.

As a result, leading partial has more chance to independently extend and be absorbed by the opposite GB before the other two partials catch up. The other two partials will be prevented from gliding by local stress and leave a periodic structure at GB, which is composed of the same partial on every three atomic planes, shown in Fig. 4c. The ITB equilibrium breaks down and the original zero-strain twinning nucleus disappears. This hypothesis is consistent with observations of such debris of periodic structure terminated at GBs of both ends in the Cu–10Zn sample (shown in Fig. 4d). Lower magnified inset of the GB indicates the generation of macroscopic strain as expected. Fig. 4e is the FFT of the selected region in Fig. 4d, further confirming the same periodic structure in Fig. 3e. The final structure of this process may not be exactly the same as stage C because extended leading partial may interact with other existing defects on the way [22]. Lower SFE makes this “move-drag” propagation less favorable and statistically reduces the proportion of zero-strain twins, as shown in Fig. 2. On the other hand, even for the lowest SFE in Cu–30Zn, there’s still considerable proportion of zero-strain twins during deformation. It seems SFE doesn’t affect the proportion so “significantly” in Fig. 2. This is reasonable because lower SFE only influences CSTP mechanism while RAP is still free to operate in NC materials and generate zero-strain twins [10].

Note that there is possible segregation of Zn solute atoms to the GBs and stacking faults, which may be affected by the Zn concentration. If Zn segregation affects the nucleation of ITB’s or its migration, the effect should be similar for both the RAP and CSTP mechanisms. The experimental observation that the CSTP mechanism is suppressed while the RAP mechanism is not suggests that the effect of the solute segregation is less significant than the SFE effect.

Another concern is whether applied stress is sufficient to activate CSTP mechanism in our experiments. Although the net force exerted on propagating ITB is nearly zero, it still needs a threshold shear stress to start the “move-drag” process [12,23]. Logically, the threshold driving shear stress for CSTP in Cu–Zn alloys should be lower than that in Cu ( $\sim 100$  MPa) [23] since their SFEs are lower and probably comparable to that of Ag ( $< 100$  MPa) [7]. The applied shear stress is estimated from Vicker hardness (Table 1), which is calculated by dividing hardness value by an empirical coefficient [24] and Taylor factor for FCC. The applied shear stresses are  $\sim 300$  MPa in the Cu–Zn NC alloys, which are sufficient to initiate CSTP in all samples. In addition, recent study also indicates that thinner twins with thickness of a few nanometers will promote the CSTP mechanism because they have more excess energies [13]. Statistics of twin lamella thickness in observed twins are

**Table 1**

Experimental applied shear stress, stacking-fault energy, observed average twin thickness in NC Cu–Zn alloys [7,18,23,25].

Materials	Cu10Zn	Cu15Zn	Cu30Zn	Cu	Ag
SFE (mJ/m <sup>2</sup> )	35	25	14	45	16
Stress (MPa)		Applied shear stress		Stress to initiate CAP	
	275	291	334	$\sim 100$	$< 100$
Twin thickness (nm)	4.1	3.7	3.1		

listed in Table 1. Clearly, average twin thickness in all materials are 3–4 nm with only a slight change.

In summary, lower SFE will decrease the fraction of zero-strain twins. This observation is attributed to the weakening of the CSTP mechanism for zero-strain deformation twinning based on observation of atomic structures of ITB. Lower SFE has statistically more chance to induce the breakdown of stress balance between partials, which deactivates CSTP mechanism and therefore leads to lower fraction of zero-strain twins.

This work is supported by the US National Science Foundation (Grant #DMT-1104667). The authors acknowledge the use of Analytical Instrumentation Facility (AIF) at North Carolina State University, which is supported by the State of North Carolina and the National Science Foundation. Y.T. Zhu also acknowledges the support of the China Thousand Talents Plan program.

## References

- [1] J.W. Christian, S. Mahajan, *Prog. Mater. Sci.* 39 (1995) 1–157.
- [2] Y.T. Zhu, X.Z. Liao, X.L. Wu, *Prog. Mater. Sci.* 57 (2012) 1–62.
- [3] A. Ookawa, *J. Phys. Soc. Jpn.* 12 (1957) 825.
- [4] J.A. Venables, *Philos. Mag.* 6 (1961) 379–396.
- [5] M. Niewczas, G. Saada, *Philos. Mag.* A 82 (2002) 167–191.
- [6] X.L. Wu, X.Z. Liao, S.G. Srinivasan, F. Zhou, E.J. Lavernia, R.Z. Valiev, Y.T. Zhu, *Phys. Rev. Lett.* 100 (2008) 095701.
- [7] L. Liu, J. Wang, S.K. Gong, S.X. Mao, *Phys. Rev. Lett.* 106 (2011) 175504.
- [8] J.Y. Zhang, P. Zhang, R.H. Wang, G. Liu, G.J. Zhang, J. Sun, *Phys. Rev. B* 86 (2012) 064110.
- [9] X.H. An, M. Song, Y. Huang, X.Z. Liao, S.P. Ringer, T.G. Langdon, Y.T. Zhu, *Scr. Mater.* 72–73 (2014) 35–38.
- [10] F. Wu, Y.T. Zhu, J. Narayan, *Mater. Res. Lett.* 2 (2014) 63–69.
- [11] Y.J. Xu, K. Du, C.Y. Cui, H.Q. Ye, *Scr. Mater.* 77 (2014) 71–74.
- [12] J. Wang, A. Misra, J.P. Hirth, *Phys. Rev. B* 83 (2011) 064106.
- [13] J. Wang, N. Li, O. Anderoglu, X. Zhang, A. Misra, J.Y. Huang, J.P. Hirth, *Acta Mater.* 58 (2010) 2262–2270.
- [14] Y.M. Wang, F. Sansoz, T. LaGrange, R.T. Ott, J. Marian, T.W. Barbee Jr., A.V. Hamza, *Nat. Mater.* 12 (2013) 697–702.
- [15] Y.T. Zhu, X.L. Wu, X.Z. Liao, J. Narayan, S.N. Mathaudhu, L.J. Kecskés, *Appl. Phys. Lett.* 95 (2009) 031909.
- [16] J. Wang, O. Anderoglu, J.P. Hirth, A. Misra, X. Zhang, *Appl. Phys. Lett.* 95 (2009) 021908.
- [17] B.Q. Li, B. Li, Y.B. Wang, M.L. Sui, E. Ma, *Scr. Mater.* 64 (2011) 852–855.
- [18] P.c. Gallaghe, *Metall. Trans.* 1 (1970) 2429.
- [19] X.L. Ma, W.Z. Xu, H. Zhou, J.A. Moering, J. Narayan, Y.T. Zhu, *Philos. Mag.* 95 (2015) 301–310.
- [20] I.J. Beyerlein, X. Zhang, A. Misra, *Annu. Rev. Mater. Res.* 44 (2014) 329–363.
- [21] J.Y. Huang, Y.T. Zhu, H. Jiang, T.C. Lowe, *Acta Mater.* 49 (2001) 1497–1505.
- [22] Y.T. Zhu, X.L. Wu, X.Z. Liao, J. Narayan, L.J. Kecskés, S.N. Mathaudhu, *Acta Mater.* 59 (2011) 812–821.
- [23] Y. Liu, J. Jian, Y. Chen, H. Wang, X. Zhang, *Appl. Phys. Lett.* 104 (2014) 231910.
- [24] G. Sundararajan, Y. Tirupataiah, *Bull. Mater. Sci.* 17 (1994) 747–770.
- [25] J.P. Hirth, J. Lothe, *Theory of Dislocations*, Wiley, 1982.